

Reversible solid-oxide cell stack based power-to-x-to-power systems: Economic potential evaluated via plant capital-cost target

Yumeng Zhang^{a,b}, Ningling Wang^b, Xiaofeng Tong^a, Liqiang Duan^b, Tzu-En Lin^c, François Maréchal^d, Jan Van herle^e, Ligang Wang^{a,f,*}, Yongping Yang^{f,*}

^a Innovation Research Institute of Energy and Power, North China Electric Power University, Beijing, China

^b National Research Center for Thermal Power Engineering and Technology, North China Electric Power University, Beijing, China

^c Institute of Biomedical Engineering, National Chiao Tung University, China

^d Industrial Process and Energy Systems Engineering, Swiss Federal Institute of Technology in Lausanne, Sion, Switzerland

^e Group of Energy Materials, Swiss Federal Institute of Technology in Lausanne, Sion, Switzerland

^f Key Laboratory of Power Station Energy Transfer Conversion and System (North China Electric Power University), Ministry of Education, China

HIGHLIGHTS

- A decomposition-based method for optimally deploying dual-direction solid-oxide stack-based plants.
- Economic feasibility evaluated for the plant concepts enabled by H₂, CH₄, CH₃OH, syngas and NH₃.
- Plant CAPEX target representing economic feasibility evaluated for multiple scenarios.
- By reducing onsite storage via the market, economic feasibility ranked as H₂ > syngas > CH₄ > CH₃OH > NH₃.
- With no chemical sale, hydrogen, methanol and ammonia pathways no longer economically feasible.

ARTICLE INFO

Keywords:

Reversible solid-oxide technology
Power-to-x-to-power
Grid balancing
Economic feasibility
Plant CAPEX target

ABSTRACT

Electrical energy storage systems are indispensable for the electrical grid with high penetration renewables. Reversible solid-oxide cell stack based power-to-x-to-power systems, which can switch between power generation and power storage, can achieve a high round-trip efficiency and are technology neutral for, e.g., hydrogen, methane, methanol, ammonia and syngas. This paper evaluates, with a systematically decomposition-based optimization method, the economic feasibility of such dual-direction plants to assist wind farms for reliable electricity supply, under various scenarios with 150%/200%/250% wind electricity penetration and strong/weak interactions with chemical markets. The economic feasibility is represented by *Plant CAPEX Target* (€/ref-stack), defined as maximum affordable total plant investment costs divided by the equivalent number of reference stacks (5120 cm² active cell area). The results show that, with strong interaction with chemical markets, hydrogen pathway is the most economically potential, especially under high wind electricity penetration (200, 250%). Plant CAPEX target of hydrogen pathway reaches 2300 €/ref-stack, followed by syngas (1900 €/ref-stack), while the methane, methanol and ammonia ones are less economically-feasible with targets around 1000 €/ref-stack. Economic feasibility of hydrogen pathway is less sensitive (above 2000 €/ref-stack) to hydrogen price when it is below 4 €/kg. Deploying multiple plants with operation-coordination freedom allows for the reduction of lost wind rate and the enhancement of profit. Plant designs with either high round-trip efficiency or good match with imbalance characteristics are preferred. When the chemicals produced are not sold to markets, syngas and methane pathways are more economically-feasible, with plant CAPEX target within 500–1000 €/ref-stack due to affordable onsite fuel storage and high round-trip efficiency.

* Corresponding authors at: North China Electric Power University, China.

E-mail addresses: ligang.wang@ncepu.edu.cn (L. Wang), yyp@ncepu.edu.cn (Y. Yang).

Nomenclature	
<i>Abbreviations</i>	
CAPEX	capital expenditures
ESS	energy storage system
LHV	lower heat value
PowGen	power generation
PowSto	power storage
PXP	power-to-x-to-power
Ref-stack	reference stack
RT	round-trip
RSOC	reversible solid-oxide cell
<i>Mathematical symbols</i>	
Cap	capacity
ND	the number of designs
F	flow
f	sizing factor
j	index of year
k	stable power generation/storage level
L	tank level
m	tank capacity
N	number of selected reversible solid-oxide cell plant
P	power
R	revenue/cost
r	ramp up/down rate
n	discount rate
S	Status of plant selection
t	startup/shut down time
TD	the number of typical days
Y	plant status
Z	plant start-up status
τ	plant lifespan
α	repetition times
θ	price
<i>Subscripts/Superscripts</i>	
af	available factor
c	index of chemical
chem	chemical
con	consumption
curt	curtailed power
d	index of plant design
D	design
elec	electricity
i	index of hours
imb	imbalance
pro	production
rd	ramp down
ru	ramp up
td	index of typical day
u	index of plant

1. Introduction

The vigorous developed renewable energies can contribute significantly to energy sustainability and environmental protection; however, it also leads to grid instability due to, e.g., power quality issues [1]. High penetration of renewables is expected to be better addressed by employing energy storage systems (ESSs), which reduce the imbalance between power generation and demand via storing excess or unexpected power and releasing it when needed [2]. The energy-storage demand worldwide will hit 266 GW [3] in 2030 (compared to 183 GW in 2019) to meet the target of 45% power generated from renewables [4]. However, the deployment of mature storage technologies, e.g., pump hydro storage and compressed air storage, suffers from either the limited geological sites or high exergy-destruction and losses. Thus, other potential energy storage technologies are currently actively explored. The lithium-ion battery is predicted to be dominating with a contribution of 150 GW in 2030 [5] due to its high energy density and round-trip efficiency (70%–80%) [6]. However, it is not capable of meeting the need for long-term electricity storage. Hydrogen-based energy storage is another promising alternative by storing electric energy to chemical energy for short- or long-term storage. For example, over 20% of Danish electricity will be converted to hydrogen or hydrogen-based fuels (power-to-x) after building a 10 GW offshore wind plant for a 70% CO₂ reduction target in 2030 [7]. The increased use of hydrogen or hydrogen-based fuels enables the decarbonization of portable, transportation and stationary sectors.

Renewable power can be converted to hydrogen via electrolysis, while in turn, the hydrogen stored can be converted to electricity via fuel cell. This whole energy storage and release process chain can be called as a power-to-x-to-power (PXP) system. Compared with conventional PXP systems using separate fuel cell and electrolyzer, the unitized fuel cells, which can switch between fuel cell mode and electrolysis mode by one single stack, could potentially reduce the capital cost due to enhanced annual utilization hours [8,9]. State-of-the-art unitized fuel cells mainly include unitized regenerative alkaline fuel cell, unitized proton exchange membrane fuel cell, and reversible solid oxide fuel cell. The

unitized low-temperature fuel cells may be hindered mainly by (1) CO₂ poisoning or imperfect membrane [9], (2) low lifetime when coupling with intermittent renewables with frequently switching between fuel cell and electrolysis [10], (3) expensive cell components due to noble metal catalysts, gas diffusion layer, and (4) low round-trip (RT) efficiency (40%–50% based on lower heat value, LHV) [11]. Instead, a reversible solid oxide fuel cell (RSOC) can potentially (1) reduce the electrolysis-induced degradation to realize a prolonged lifespan [12], (2) reach low capital investment costs due to no use of precious and expensive metal catalysts [13], and (3) achieve high RT efficiency of 55%–70% (LHV) [14]. Thus, the RSOC based PXP systems are attractive to cope with the imbalance between power generation and demand.

There have been several applications of the hydrogen and methane based PXP systems. For example, a grid-connected RSOC system with 50 kW in power generation (PowGen) mode and 120 kW in power storage (PowSto) mode has been employed for the stabilization of a microgrid by Sunfire and Boeing [15] with the interactions among multi-market segments including hydrogen production, energy storage and grid balancing. The system was successfully operated with micro-grid connection for over 1000 h although experiencing several abrupt shut-downs. Sunfire also installed an RSOC plant prototype in Salzgitter to produce hydrogen for iron-and-steel works when renewable electricity is sufficient or to supply power when the electricity price is high [16]. An RT efficiency of 50% (LHV) was achieved under steady-state, full-load operation [16]. By storing water–vapor containing gas mixture rather than condensed water separately to reduce the heat required for steam generation for electrolysis, a 100 kW-scale RSOC methane-based system can achieve an RT efficiency of nearly 74% [23]. Even with 15% of rated capacity, an RT efficiency of 44% is still viable [17].

The large-scale deployment of RSOC-based dual-direction plants is currently limited by economic feasibility. The installed capital expenditures (CAPEX) of an RSOC-based dual-direction system converted from Ref. [18] is 1850 \$/ref-stack with the reference stack defined as the electrode-supported cell stack with an active cell area of 5120 cm². The levelized cost of energy with 5694-hour annual operation is estimated to be 20 ¢/kWh without coupling with a real application, i.e., operating at

rated power and storage [17], which is almost double of that of pumped hydro energy storage [19]. When reducing the CAPEX down to 1200 \$/ref-stack (5120 cm²/ref-stack), the levelized energy cost with 5694-hour annual operation can be decreased to 11 ¢/kWh [17], reaching the level of pumped hydro technology. Thus, the CAPEX of the RSOC-based system needs to be reduced for commercial applications [20,18], for which varying the plant design (energy efficiency and density) is helpful [21,22]. There are trade-offs between efficiency, gas storage sizes and CAPEX [23], thus the maximum RT efficiency differs from the lowest CAPEX system due to large intermediate gas storage tanks [24,25]. For the plants with the same stack size, there can be a number of plant design alternatives realizing different capacity (energy density) and efficiency for power generation, power storage and gas storage [25]. With a set of plant designs, the optimal plant size (and CAPEX) to cope with a specific power imbalance profile might vary significantly [26].

There were only limited studies on the economic feasibility of coupling RSOC plants with renewables. The payback time of a hydrogen-based RSOC system was concluded to be close to the stack lifespan when the plant worked with an average of 50% load factor [27], and became even worse when considering start-up and part-load operation [27,28]. The literature has not identified, in a sufficient manner, the economic feasibility of such RSOC-based plants, since they disovered the optimal RSOC plant design and system deployment under a fixed plant size [29,30], or optimized plant size with a limited number of design alternatives [28,29]. Only one single plant was considered in the literature without considering the coordinative operation of multiple plants installed with varied thermodynamic performances and different plant sizes to better address the imbalance profiles. Moreover, the literature only investigated the economic feasibility of the hydrogen and methane based RSOC plants, while those realized by other chemicals, e.g., methanol, ammonia and syngas, have never been investigated.

The objective of this work is to investigate, in a comprehensive manner, the economic feasibility of RSOC dual-direction plants combining both technological and application viewpoints. The maximum affordable plant CAPEX is evaluated by considering (1) a number of plant concepts (process chains) realized by different chemicals, (2) a number of plant design alternatives, (3) optimal plant sizing and scheduling with different plant designs, (4) a number of application scenarios, and (5) sensitivity analysis of key influential factors. This paper is a follow-up of our previous study [25], which proposed a decomposition-based two-step optimization method for the optimal deployment of RSOC plants and investigated thermodynamic performances of the RSOC process chains based on hydrogen, methane, methanol, syngas and ammonia, thus creating an application-free pool of optimal plant designs for each process chain. The two-step optimization method proposed before is further enhanced and put into practice in this paper.

The remaining paper is organized as follows: In Section 2, the RSOC based energy storage system is introduced with the description of dual-direction RSOC plant concept and design pool. Then, the extended

optimal deployment methodology to identify potential business cases of RSOC based energy storage system is described in Section 3. Section 4 describes the application of coping RSOC with renewables in detail with the specifications and assumptions. The economic feasibility is further discussed comprehensively in Section 5 to draw the conclusions in Section 6.

2. Concept and design pool of dual-direction RSOC plant

2.1. Concept of dual-direction plant

Five power-to-x-to-power process chains enabled by different chemicals (hydrogen, ammonia, syngas, methane, and methanol) were studied and compared in Ref. [25]:

1. Hydrogen pathway via steam electrolysis: power-to-hydrogen-to-power
2. Ammonia pathway via steam electrolysis: power-to-ammonia-to-power
3. Syngas pathway via co-electrolysis of steam and carbon dioxide (CO₂): power-to-syngas-to-power
4. Methane pathway via steam electrolysis: power-to-hydrogen-to-methane-to-power
5. Methanol pathway via stem electrolysis: power-to-hydrogen-to-methanol-to-power

The dual-direction plants can switch between PowGen and PowSto modes with the aid of intermediate storage tanks, as illustrated in Fig. 1. In the PowGen mode, fuels are electrochemically oxidized by pure oxygen to produce electricity with the exhaust gas (CO₂ or N₂) stored in exhaust tanks. In the PowSto mode, the steam is electrolyzed to hydrogen, which may be further converted to chemical products for the PowGen mode. The management of mass storage tanks for the continuous operation depends on practical applications. When evaluating the system thermodynamic performance, the power consumed to pressurize the chemicals for storage is considered. The pressures of chemicals storage tanks are referred to Ref. [25].

2.2. Design pool of dual-direction plant

The design pool of this dual-direction RSOC plant concept has been generated in our previous study [25], which contains a set of optimal design alternatives for different process chains. Design candidates were generated at first by (1) varying the key operating variables of the stack as well as chemical reactors of different processes, and (2) optimizing the heat cascade utilization. Then, the optimal design alternatives were evaluated for multiple objective functions including the round-trip efficiency and power densities of both modes. The optimal plant designs in the pool represent the trade-offs between the three objectives, thus with the same size of stacks, the plant can interact with the grid and market at different capacities.

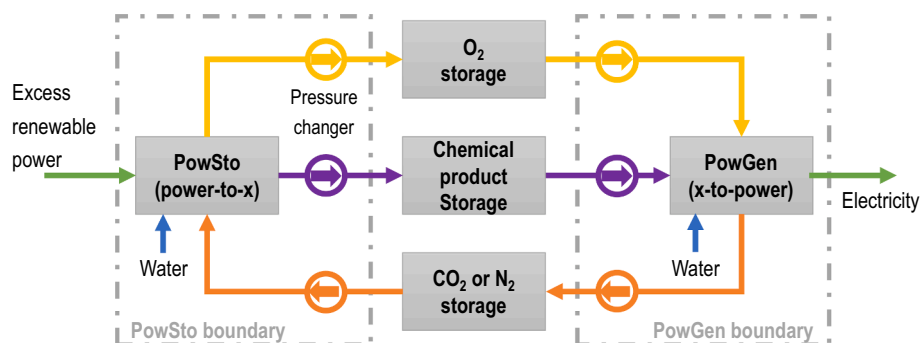


Fig. 1. The general schematic and system boundaries of the dual-direction RSOC plant [25].

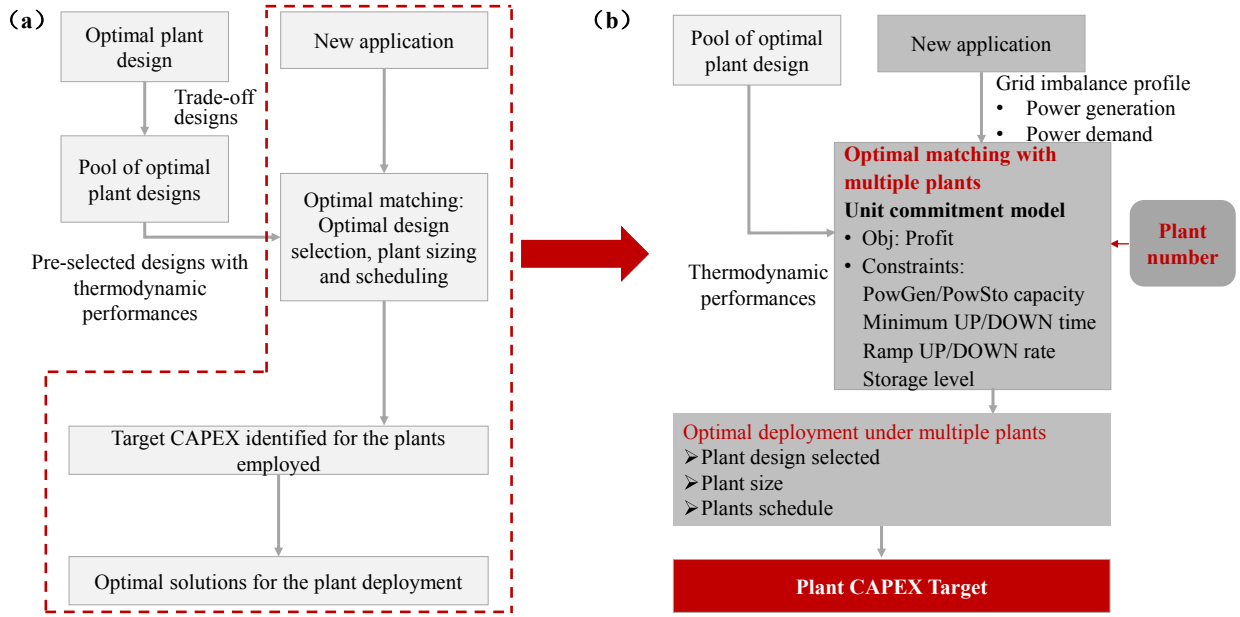


Fig. 2. Optimal deployment of the RSOC plants for specific applications: (a) the decomposition-based two-step optimization method proposed in Ref. [25], (b) the extended optimal deployment methodology of multiple plants.

3. Method of economic feasibility evaluation

3.1. Extended optimal deployment methodology to identify potential business cases

The decomposition-based two-step optimal deployment method originally proposed by the authors (Fig. 2(a)) is further extended as shown in Fig. 2(b) to assist the identification of potential business cases. By optimal matching the plant design for specific applications, the imbalance can be best handled by the coordination of multiple RSOC-based plants. The profits from imbalance handling and chemical trade are maximized by proper sizing and scheduling of different plants with varied plant designs and sizes. The optimal scheduling considers the PowGen/PowSto capacity limits, ramp up/down rates, start-up/shutdown times, and the storage level of chemical tanks. The solving of the optimal matching problem under multiple plants results in (1) specific plant designs selected, (2) optimal sizes of each plant and chemical tank, and (3) optimal scheduling of each plant employed. Then, the economic indicator, *Plant CAPEX Target* (€/ref-stack) in payback time l years, defined as the maximum affordable total plant investment costs divided by the equivalent number of reference stacks (ref-stack, each with 5120 cm² active cell area), can be calculated:

3.2.1. Objective function

The profit of RSOC based energy storage systems obtained in l years, as given in Eq. (2), is affected by (1) the revenue from increased electricity sale ($R_{td,i}^{elec}$) due to the accommodation of additional renewable energy, (2) the revenue from reduced imbalance costs ($R_{td,i}^{imb}$), (3) additional revenue (positive) or cost (negative) of chemical trade with the market ($R_{td,i}^{chem}$), (4) the costs of chemical storage tank (R^{tank}), and (5) the plant startup cost ($R_{td,i}^{start}$):

$$Profit(l) = \sum_{j=1}^l \sum_{td=1}^{TD} \alpha_{td} \left[\frac{(R_{td,i}^{elec} - R_{td,i}^{elec,0}) + (R_{td,i}^{imb,0} - R_{td,i}^{imb}) + R_{td,i}^{chem} - R_{td,i}^{start}}{(1+n)^l} \right] - R^{tank} \quad (2)$$

where the payback years l should be shorter than the stack lifespan τ , TD is the number of typical days td representing long-term historical data [37], α_{td} is the repetition times of each typical day in an entire year, i represents the hours (1–24 h) in each typical day, n is the discount rate (0.05).

The revenue of electricity sale (€/year) can be calculated as:

$$Plant \ CAPEX \ target \ (l) = \frac{\text{Maximum profit over the lifetime } (l)}{\text{Total number of reference stacks of all plants installed}} \quad (1)$$

3.2. Formulations of optimal design selection, plant sizing and scheduling

The profit of the RSOC based energy storage system is derived with a base case where no RSOC plant is installed. The investment and O&M costs of the renewable power plants themselves are not considered in all cases since these costs remain the same.

$$R_{td,i}^{elec} = \theta^{elec} (P_{td,i}^{load} - P_{td,i}^{imb}) \quad (3)$$

where θ^{elec} (€/MWh) is the electricity price, the $P_{td,i}^{load}$ (MW) is load demand in the time step i of the typical day td , and the $P_{td,i}^{imb}$ (MW) represents the part that imbalanced.

The imbalance costs $R_{td,i}^{imb}$ can be calculated by using the imbalance power and the imbalance price (θ^{imb} , €/MWh):

$$R_{td,i}^{\text{imb}} = P_{td,i}^{\text{imb}} \theta^{\text{imb}} \quad (4)$$

The revenue from chemical trade $R_{td,i}^{\text{chem}}$ is calculated as the chemical sale income minus chemical purchase costs:

$$R_{td,i}^{\text{chem}} = \sum_c (\theta_c^{\text{out}} F_{c,td,i}^{\text{out}} - \theta_c^{\text{in}} F_{c,td,i}^{\text{in}}) \quad (5)$$

where the $F_{c,td,i}^{\text{out}}$ (kg/h) represents the outflow of chemical c from chemical storage tanks to the market at typical day td , time step i ; Oppositely, the $F_{c,td,i}^{\text{in}}$ (kg/h) represents the inflow of chemical c . The θ_c^{out} and θ_c^{in} (€/kg) are the prices of chemical sale and chemical purchase respectively.

The startup costs $R_{td,i}^{\text{start}}$ (€) of the plant are considerable: Around 1.3 kWh of energy is needed for the cold-start of a 1 kW stack [31]. The startup costs are evaluated by the related energy costs:

$$R_{td,i}^{\text{start}} = \sum_d^{ND} 1.3 \theta^{\text{elec}} f_d \text{Cap}_d^{\text{PowGen,D}} Z_{d,td,i} \quad (6)$$

where d represents the RSOC plant design with a given size in the design pool, with PowGen capacity $\text{Cap}_d^{\text{PowGen,D}}$ (MW), f_d (-) is the sizing factor of design d referring to the given size. The binary variable $Z_{d,td,i}$ represents the plant start-up status:

$$Z_{d,td,i} \geq (Y_{d,td,i}^{\text{PowGen}} + Y_{d,td,i}^{\text{PowSto}}) - (Y_{d,td,i-1}^{\text{PowGen}} + Y_{d,td,i-1}^{\text{PowSto}}) \quad (7)$$

where, the binary variables $Y_{d,td,i}^{\text{PowGen}}$ and $Y_{d,td,i}^{\text{PowSto}}$ represent the status of PowGen mode and PowSto mode, respectively.

The costs of chemical storage tanks R^{tank} (€) is calculated by the tank capacity m_c (kg) and the tank price θ_c^{tank} (€/kg) of chemical c :

$$R^{\text{tank}} = \sum_c \theta_c^{\text{tank}} m_c \quad (8)$$

3.2.2. Constraints

3.2.2.1. Power balance constraints. The main constraint is the supply–demand balance. For each time step (td, i), the load demand $P_{td,i}^{\text{load}}$ (MW) is to be met by the power generation of the PowGen mode $P_{u,td,i}^{\text{PowGen}}$ (MW). However, when the demand cannot be fully met, there exists an imbalanced power $P_{td,i}^{\text{imb}}$ (MW). If there is excess electricity, it will be first stored by the power consumed of the PowSto mode $P_{d,td,i}^{\text{PowSto}}$ (MW), while the part beyond the PowSto capacity will be curtailed ($P_{td,i}^{\text{curt}}$, MW). Thus, the supply–demand balance is expressed as below:

$$P_{td,i}^{\text{load}} - P_{td,i}^{\text{imb}} = \sum_u P_{u,td,i}^{\text{PowGen}} - \sum_d P_{d,td,i}^{\text{PowSto}} - P_{td,i}^{\text{curt}} \quad (9)$$

where the set u represents renewable power plants and the RSOC-based plants, $d \subseteq u$. For off-grid applications or power systems with reliability requirement, the supply–demand imbalance is strictly not allowed:

$$P_{td,i}^{\text{imb}} = 0 \quad (10)$$

3.2.2.2. Power generation constraints. The power generation of the employed plants at each time is limited by its power capacity:

$$P_{u,td,i}^{\text{PowGen}} \leq f_{u,td,i}^{\text{af}} Y_{u,td,i}^{\text{PowGen}} \text{Cap}_u^{\text{PowGen}} \quad (11)$$

where the available factor $f_{u,td,i}^{\text{af}}$ (%) is used to define the maximum time-dependent power generation level of renewable power plants, which depends on wind or solar conditions. It is one for the RSOC-based dual-direction plants.

The PowGen capacity $\text{Cap}_d^{\text{PowGen}}$ (MW) of the actual RSOC plant employed plant design d is calculated by the design PowGen capacity

($\text{Cap}_d^{\text{PowGen,D}}$) and a sizing factor f_d :

$$\text{Cap}_d^{\text{PowGen}} = f_d \text{Cap}_d^{\text{PowGen,D}} \quad (12)$$

Therefore, the actual plant employed is sized from the preselected design by a factor of f_d . The power output of the RSOC-based plant should be over the stable generation level k_d^{PowGen} if committed:

$$P_{d,td,i}^{\text{PowGen}} \geq k_d^{\text{PowGen}} Y_{d,td,i}^{\text{PowGen}} \text{Cap}_d^{\text{PowGen}} \quad (13)$$

The plant power output at the time (td, i) is also related to that in the previous hour ($td, i-1$) and the ramp-up/down rates ($r_d^{\text{ru,PowGen}}, r_d^{\text{rd,PowGen}}$) to settle down on another steady state:

$$P_{d,td,i}^{\text{PowGen}} - P_{d,td,i-1}^{\text{PowGen}} \leq r_d^{\text{ru,PowGen}} \text{Cap}_d^{\text{PowGen}} \quad (14)$$

$$P_{d,td,i-1}^{\text{PowGen}} - P_{d,td,i}^{\text{PowGen}} \leq r_d^{\text{rd,PowGen}} \text{Cap}_d^{\text{PowGen}} \quad (15)$$

3.2.2.3. Power storage constraints. Similar to the power generation constraints, the actual power storage ($P_{d,td,i}^{\text{PowSto}}$, MW) is limited by the capacity ($\text{Cap}_d^{\text{PowSto}}$, MW) and stable level k_d^{PowSto} (-):

$$P_{d,td,i}^{\text{PowSto}} \leq U_{d,td,i}^{\text{PowSto}} \text{Cap}_d^{\text{PowSto}} \quad (16)$$

$$P_{d,td,i}^{\text{PowSto}} \geq k_d^{\text{PowSto}} Y_{d,td,i}^{\text{PowSto}} \text{Cap}_d^{\text{PowSto}} \quad (17)$$

The PowSto capacity $\text{Cap}_d^{\text{PowSto}}$ (MW) of actual RSOC plant is calculated by PowSto capacity of the plant design ($\text{Cap}_d^{\text{PowSto,D}}$, MW) and the sizing factor f_d

$$\text{Cap}_d^{\text{PowSto}} = \text{Cap}_d^{\text{PowSto,D}} f_d \quad (18)$$

The power charging to the RSOC plants is limited by the ramp-up/down rates:

$$P_{d,td,i}^{\text{PowSto}} - P_{d,td,i-1}^{\text{PowSto}} \leq \text{Cap}_d^{\text{PowSto}} r_d^{\text{ru,PowSto}} \quad (19)$$

$$P_{d,td,i-1}^{\text{PowSto}} - P_{d,td,i}^{\text{PowSto}} \leq \text{Cap}_d^{\text{PowSto}} r_d^{\text{rd,PowSto}} \quad (20)$$

The storage level $L_{c,td,i}$ (kg) of a chemical storage tank is limited by the tank capacity m_c (kg):

$$L_{g,td,i} \leq m_c \quad (21)$$

The storage level $L_{c,td,i}$ in time (td, i) is related to that in the previous hour ($td, i-1$), the chemical produced/consumed by the RSOC plants ($F_{d,c,td,i}^{\text{pro}}/F_{d,c,td,i}^{\text{con}}$, kg/h) and traded with the market ($F_{c,td,i}^{\text{in}}/F_{c,td,i}^{\text{out}}$, kg/h):

$$L_{c,td,i} = L_{c,td,i-1} + \sum_d (F_{d,c,td,i}^{\text{pro}} - F_{d,c,td,i}^{\text{con}}) + F_{c,td,i}^{\text{in}} - F_{c,td,i}^{\text{out}} \quad (22)$$

The chemical production/consumption is correlated to the power generation and storage ($P_{d,td,i}^{\text{PowGen}}, P_{d,td,i}^{\text{PowSto}}$) of the RSOC plant:

$$F_{d,c,td,i}^{\text{pro}} = P_{d,td,i}^{\text{PowGen}} \frac{F_{d,c}^{\text{PowGen,pro,D}}}{\text{Cap}_d^{\text{PowGen,D}}} + P_{d,td,i}^{\text{PowSto}} \frac{F_{d,c}^{\text{PowSto,pro,D}}}{\text{Cap}_d^{\text{PowSto,D}}} \quad (23)$$

$$F_{d,c,td,i}^{\text{con}} = P_{d,td,i}^{\text{PowGen}} \frac{F_{d,c}^{\text{PowGen,con,D}}}{\text{Cap}_d^{\text{PowGen,D}}} + P_{d,td,i}^{\text{PowSto}} \frac{F_{d,c}^{\text{PowSto,con,D}}}{\text{Cap}_d^{\text{PowSto,D}}} \quad (24)$$

where $F_{d,c}^{\text{PowGen,pro,D}}$ and $F_{d,c}^{\text{PowSto,pro,D}}$ are the production of chemical c from the plant design d in PowGen and PowSto modes, while $F_{d,c}^{\text{PowGen,con,D}}$ and $F_{d,c}^{\text{PowSto,con,D}}$ are the consumption of chemical c in both modes.

The optimization is carried out with the aid of typical days to reduce the computational efforts. The scheduling of the plants on each typical day is independent. Thus, the storage levels in the first and the last hour in each typical day are set to be equal for continuous operation of the storage tanks:

$$L_{c,td,i=1} = L_{c,td,i=24} \quad (25)$$

The number (N) of the RSOC-based plants employed is specified by the summation of binary variables S_d , which represents whether the plant design d is selected or not:

$$S_d \geq Y_{d,td,i}^{\text{PowGen}} + Y_{d,td,i}^{\text{PowSto}} \quad (26)$$

$$\sum_d S_d = N \quad (27)$$

3.2.2.4. Minimum up and down time. Several components of the RSOC based plant operate at a high temperature of over 600 °C, thus the plant needs time (up to several hours) to start up and shut down [32]. This will affect the plant's interaction with the electrical grid. Thus, the startup and shutdown are considered by employing specified t^{su} (h) and t^{sd} (h):

$$\sum_{ii=i}^{i+t^{\text{su}}-1} Y_{d,td,ii}^{\text{PowGen}} \geq t^{\text{su}} (Y_{d,td,i}^{\text{PowGen}} - Y_{d,td,i-1}^{\text{PowGen}}) \quad (28)$$

$$\sum_{ii=i}^{i+t^{\text{sd}}-1} Y_{d,td,ii}^{\text{PowSto}} \geq t^{\text{sd}} (Y_{d,td,i}^{\text{PowSto}} - Y_{d,td,i-1}^{\text{PowSto}}) \quad (29)$$

$$\sum_{ii}^{i+t^{\text{sd}}-1} (1 - Y_{d,td,ii}^{\text{PowGen}}) \geq t^{\text{sd}} (Y_{d,td,i-1}^{\text{PowGen}} - Y_{d,td,i}^{\text{PowGen}}) \quad (30)$$

$$\sum_{ii}^{i+t^{\text{su}}-1} (1 - Y_{d,td,ii}^{\text{PowSto}}) \geq t^{\text{su}} (Y_{d,td,i-1}^{\text{PowSto}} - Y_{d,td,i}^{\text{PowSto}}) \quad (31)$$

4. Application and specifications

4.1. Application description

The application investigated as schematically shown in Fig. 3 is to address the power imbalance related to a local power grid supporting Sicily, Sardinia and South of Italy. Major renewable energy involved is from a wind farm. The RSOC-based dual-direction plants are expected to serve as a power supplier to complement the power shortage by converting fuels to electricity in the PowGen mode (red lines), or as a power consumer to store excess wind power in the PowSto mode (blue lines). This power system has reliability requirement i.e., all the load demand should be satisfied (Eq. (10)). The chemical trade with the market is managed to keep the continuous operation of fuel tanks with the enhancement of plant revenue. The interactions with the market are defined at two levels: (a) strong or (b) weak. The former stands for an easy access to the market, allowing for daily trades of chemicals and thus a reduction of the tank sizes. The latter stands for a limited interaction

with the market, thus the onsite storage tanks will be large to allow for continuous switch between two modes.

The electrical grid of the application transmits 300 GWh electricity per year with data available from 01.01.2018 to 31.12.2018 on an hourly basis. The 16 MW wind power plant installed supplies 33 GWh electricity in 2010. To find the prerequisites for potential business cases, the wind power capacity is scaled up to 165 MW and 220 MW, corresponding to a wind electricity penetration of 150% and 200%, which is defined as the annual wind electricity generated divided by the gross annual electricity demand. The hourly profiles of power demand and wind power (365 days, 8760 values) are clustered into 8 typical days using the k -means developed in Ref. [33].

4.2. Design preselection from the design pool

The design pool for each PXP process chain is pre-selected from the Pareto fronts obtained in our previous study [25]. Each design pool contains 31 RSOC plants, which are evenly selected from hundreds of optimal designs generated. As an example, the design pool of hydrogen based RSOC plants is shown in Fig. 4. The characteristics of the plant design used for optimal deployment include:

- Specific PowGen capacity: Net system electricity generation capacity, kWe/ref-stack
- Specific PowSto capacity: Total system electricity consumption capacity, kWe/ref-stack
- The system-level balance of the materials, i.e., CO₂, O₂ and the targeted fuel/chemical, in kg/ref-stack

4.3. Specifications and assumptions

The economic parameters specified in the optimization are listed in Table 1.

5. Results and discussion

The scenario with strong interactions with the chemical markets, whose economic feasibility is less affected by the sizes of chemical storage tanks, is first discussed in Section 5.1. Then, the scenario with weak interactions with the chemical markets is investigated in Section 5.2 for, e.g., remote applications.

5.1. The scenario with strong interactions with the chemical market

5.1.1. Overview of the plant CAPEX target

By solving the optimization problem described in Section 3.2, the Plant CAPEX Target (€/ref-stack) for 5-year stack lifetime is calculated as

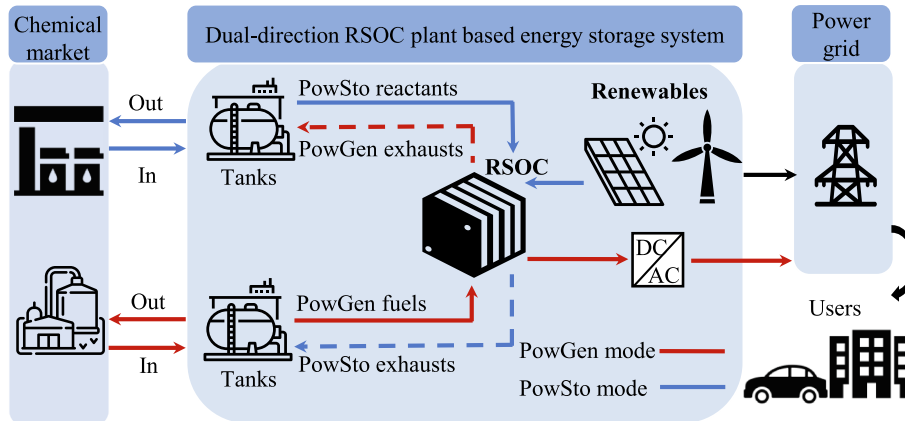


Fig. 3. Application description with either (a) strong or (b) weak interactions with the chemical market.

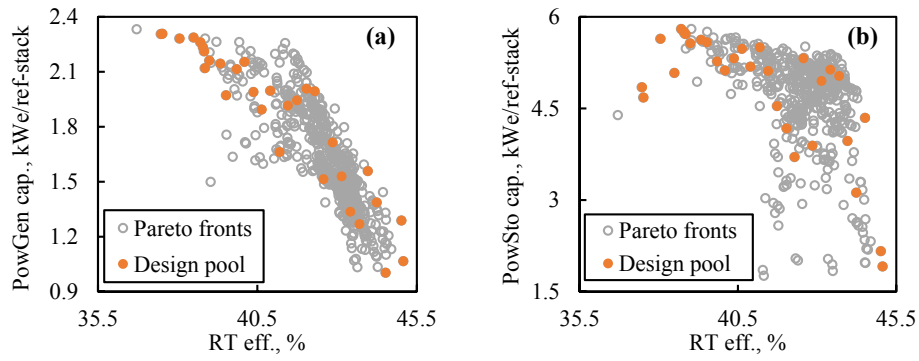


Fig. 4. Evenly selected plant designs (colored) for design pool from all optimal trade-off designs (grayed) generated in Ref. [25]: (a) RT efficiency vs PowGen capacity per reference stack; (b) RT efficiency and PowSto capacity per reference stack.

Table 1
Parameters specifications.

	Parameters	Descriptions	Units	Values	Ref.
Market prices	$\theta_{O_2}^{out}/\theta_{O_2}^{in}/\theta_{O_2}^{tank}$	O ₂ sell/buy/tank price	€/kg	0.06/0.1/8	[34]
	$\theta_{CO_2}^{out}/\theta_{CO_2}^{in}/\theta_{CO_2}^{tank}$	CO ₂ sell/buy/tank price	€/kg	0.12/0.2/6	[35]
	$\theta_{CH_4}^{out}/\theta_{CH_4}^{in}/\theta_{CH_4}^{tank}$	CH ₄ sell/buy/tank price	€/kg	0.8/1.2/14	[36]
	$\theta_{SYN}^{out}/\theta_{SYN}^{in}/\theta_{SYN}^{tank}$	SYN sell/buy/tank price	€/kg	0.36/0.54/12	
	$\theta_{MeOH}^{out}/\theta_{MeOH}^{in}/\theta_{MeOH}^{tank}$	MeOH sell/buy/tank price	€/kg	0.4/0.6/3	[34]
	$\theta_{NH_3}^{out}/\theta_{NH_3}^{in}/\theta_{NH_3}^{tank}$	NH ₃ sell/buy/tank price	€/kg	0.4/0.7/15	[37]
	$\theta_{N_2}^{out}/\theta_{N_2}^{in}/\theta_{N_2}^{tank}$	N ₂ sell/buy/tank price	€/kg	0.2/0.3/9	
	$\theta_{H_2}^{out}/\theta_{H_2}^{in}/\theta_{H_2}^{tank}$	H ₂ sell/buy/tank price	€/kg	2.7/4.0/200	[38,39]
	ρ^{elec}	Electricity price	€/MWh	40	
	ρ^{imb}	Imbalance price	€/MWh	195	[38]
RSOC plant performance	$r_{d}^{ru, PowGen} / r_{d}^{ru, PowSto}$	Ramp up rate	-	0.75	[40]
	$r_{d}^{rd, PowGen} / r_{d}^{rd, PowSto}$	Ramp down rate	-	0.75	[40]
	t^{su} / t^{sd}	Startup/ Shut down time	h	4	[40]
	$k_d^{PowGen} / k_d^{PowSto}$	PowGen/ PowSto stable level	-	0.3	[40]
	τ	RSOC plants lifespan	-	5	[41,42]

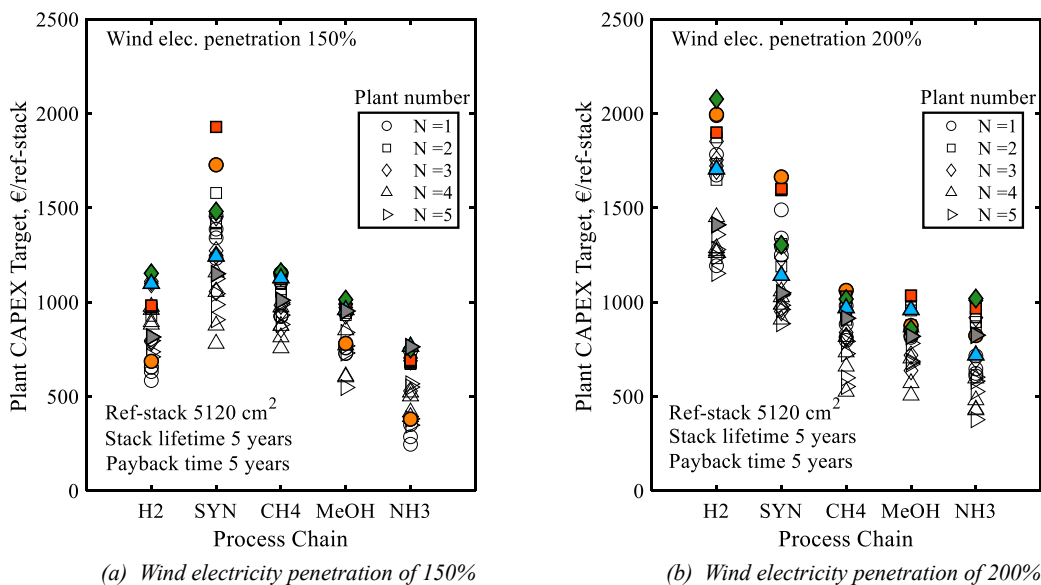


Fig. 5. Plant CAPEX targets of different process chains under various scenarios with different renewable electricity penetration, different plant numbers from 1 to 5, a stack lifetime of 5 years, and a payback time of 5 years. Integer-cut to obtain the sub-optimal solutions is performed 5 times for each process chain and scenario with the highest plant CAPEX target highlighted by the symbols filled.

shown in Fig. 5 for each PXP process chain under various scenarios with different plant numbers (1–5), different levels of renewable electricity penetration (150% and 200%). The RSOC plants should satisfy all the power shortage due to the reliability requirement of the target application (Eq. (10)). The stack lifetime is assumed to be 5 years, which is commonly viable for state-of-the-art technologies [41,42]. Overall, the plant CAPEX target ranges widely under different scenarios and reaches up to 2000 €/ref-stack for the hydrogen pathway with 3 plants and 200% wind electricity penetration. However, the plant CAPEX target of the ammonia pathway calculated can be even as low as 400 €/ref-stack under the scenario with a single plant and 150% wind electricity penetration. The methanol and ammonia process chains tend to have lower plant CAPEX target than those enabled by syngas, hydrogen, and methane, which indicates that the methanol and ammonia process chains are with lower economic feasibility.

When the wind electricity penetration reaches 150% (Fig. 5(a)), the syngas-based plant concept achieves the highest plant CAPEX of 1100–1900 €/ref-stack, followed by the methane and hydrogen based plant concept 1000–1200 and 700–1200 €/ref-stack. The methanol-based plants seem to be more difficult to be economically feasible with the plant CAPEX target being 800–1000 €/ref-stack. The lowest plant CAPEX target is still achieved by the ammonia process chain, 400–800 €/ref-stack.

For the scenarios with 200% wind electricity generation (Fig. 5(b)), the hydrogen based plant concept shows the highest economic potential with the plant CAPEX target reaching up to 1400–2100 €/ref-stack, much higher than that under 150% wind electricity penetration. The syngas case gives a slightly decreased CAPEX target of 1100–1700 €/ref-stack. A similar descending situation is also observed for the methane and methanol cases with the targets of 900–1100 €/ref-stack and 800–1000 €/ref-stack, respectively. With the increased penetration of renewable electricity, the economic feasibility of the ammonia pathway is slightly enhanced 700–1000 €/ref-stack. The difference of the plant CAPEX target under the two levels of renewable electricity penetration is further investigated in Section 5.1.3.

The number of the RSOC-based plants employed has a great influence on the plant CAPEX target. With 150% renewable electricity penetration, the highest plant CAPEX target is achieved by two or three plants, while those with one (hydrogen, methanol, ammonia) or five (syngas, methane) plants show the worst economic feasibility, i.e., the lowest CAPEX target. When increasing wind electricity penetration to 200%, using a single plant is no longer the most unaffordable case, and even becomes the most economically potential for syngas- or methane-based plants.

The plant CAPEX target is also evaluated for the scenarios with a payback time of 1–4 years, which is affected by the tank costs incurred at the first year and the sum of the reduced imbalance costs, additional

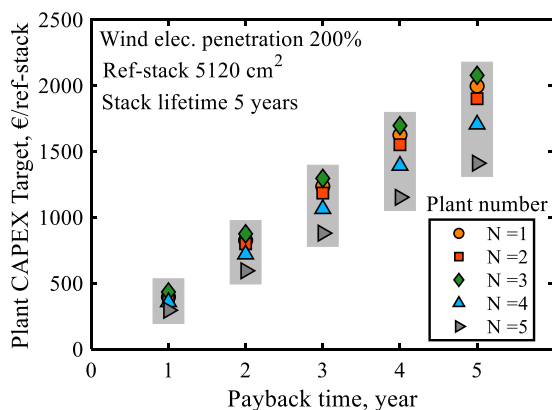


Fig. 6. Plant CAPEX target of the hydrogen process chain for the scenarios with payback time between 1 and 5 years and wind electricity penetration of 200%.

revenue or the costs related to the gas purchase and plant startup occurring before reaching the set payback year. Here the results for the case with the highest economic feasibility in Fig. 5, i.e., hydrogen pathway under 200% wind electricity penetration, is given in Fig. 6. In general, to reach a short payback time, the plant CAPEX target decreases significantly, indicating the strong need for reducing system CAPEX for high economic feasibility. For the hydrogen case, the plant CAPEX targets are reduced almost linearly from 1400 to 2100 €/ref-stack for the payback time of 5 years to 900–1300 €/ref-stack for the payback time of 3 years. Additionally, the plant CAPEX needs to be below 300–400 €/ref-stack to pay back the investment within one year.

Considering the definition of plant CAPEX target (Eqs. (1) and (2)), the major influential factors causing the above observations are (1) the plant sizes, representing the total number of reference stacks employed, (2) the lifetime income, (3) the lifetime operating costs, and (4) the investment costs of the storage tanks. However, since the last factor presents a very limited effect when with strong interactions with the chemical markets, the first three factors are further discussed below to elaborate on the plant CAPEX target difference between different plant concepts.

5.1.2. RSOC plant design selected

For each pathway with a specific plant number from one to five, five deployment solutions (cases) with one optimal solution and four sub-optimal solutions (cases) generated by integer-cut technique were obtained, thus there were 25 deployment solutions for each process chain, which deploy in total 75 plants. The plant-design repetition for the 75 plants deployed is shown in Fig. 7.

With the wind electricity penetration of 150%, the hydrogen-based process chain strongly prefers the designs with high RT efficiency, as shown in Fig. 7(a), and particularly, the design with the highest RT efficiency (45.2%) was selected in 21 cases, followed by the designs with the second and third highest RT efficiencies (45%, 44.5%) selected for 15 and 13 cases, respectively. The use frequency of these three most efficient designs accounts for over 65% of all 75 plants deployed in the 25 cases, while the designs with RT efficiency lower than 42% have never been chosen. Thus, the RT efficiency is the dominating factor for plant-design selection, while the PowGen and PowSto capacities are less important. The same situation is also observed for methane, methanol and ammonia pathways. Particularly, for the methane pathway, only the ten designs with RT efficiency of over 45% were selected, and the most efficient three designs appear 46 times out of all 75 plants deployed.

For the syngas process chain (Fig. 7(b)), the design with the highest PowSto capacity 8 kWe/ref-stack (system electricity consumption) is the most frequently selected (19 cases). Similarly, the designs with high RT efficiency are preferred, with those with the highest RT efficiencies (46.6% and 46.3%) selected in 16 and 14 cases. There is a special situation that only occurs in the syngas pathway: The design with the highest PowSto capacity but a lower RT efficiency has been selected for 19 cases. The features of this design are (1) the ratio of PowSto/PowGen capacity, enabled by a large PowSto capacity and a small PowGen capacity, better matches the imbalance profile, and (2) the PowSto efficiency is not the highest but still high (75%) due to the benefit of co-

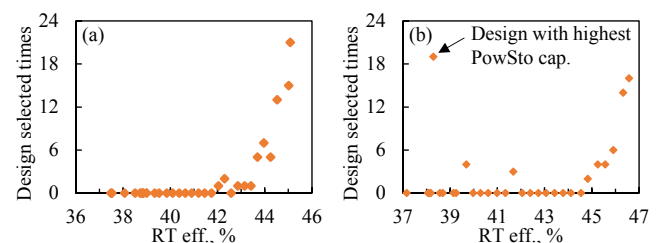


Fig. 7. Selection of designs under 150% wind electricity penetration: (a) Hydrogen based designs, (b) Syngas based designs.

electrolysis [25]. Therefore, with the same PowGen capacity, the plant with this design could convert more electricity in the PowSto mode, thus reducing the wind power curtailment. The amount of the chemical production of the PowSto mode is also affected by the PowSto efficiency. Therefore, the selection of this plant design is a result of the trade-off between increased accommodation of wind power and reduced PowSto efficiency.

Increasing wind electricity penetration to 200%, the selection of plant designs of different concepts has a similar preference as the scenario with wind electricity penetration of 150%, i.e., (1) the designs with the highest RT efficiency for the hydrogen, methane, methanol and ammonia pathways, and (2) the designs with highest PowSto capacity or high RT efficiency for the syngas pathway.

The designs selected in the cases with the highest plant CAPEX target are illustrated in Fig. 8 with the average efficiency (Fig. 8(a)) and capacity (Fig. 8(b)) of the plants deployed. The average efficiencies of the selected designs are close for the two scenarios with different wind electricity penetration (150% and 200%), because only several designs with high RT efficiency or the highest PowSto capacity (for only syngas pathway) are selected. The PowSto and PowGen efficiencies of the selected designs are within 67% (ammonia) – 80% (syngas) and 55% (syngas) – 67% (methane).

For the selected plant designs with high RT efficiency, the capacities of both modes are limited due to the trade-off between efficiency and capacity. For the scenarios with a wind electricity penetration of 150%, the PowGen capacities of the selected designs are ranked as syngas (1.3 kWe/ref-stack) > hydrogen (1.2 kWe/ref-stack) > methanol (1.1 kWe/ref-stack) > ammonia ≈ methane (1 kWe/ref-stack), while the PowSto capacities are within 3.4 (methanol) – 4 kWe/ref-stack (ammonia).

Increasing the wind electricity penetration to 200%, the PowSto capacity is increased to address the increased excess wind power by enhancing the proportion of plant designs with higher PowSto capacity, ranging from 5.4 (hydrogen) – 4.3 kWe/ref-stack (ammonia). The PowGen capacity is ranked as hydrogen (1.5 kWe/ref-stack) > syngas ≈ methane (1.3 kWe/ref-stack) > ammonia (1.2 kWe/ref-stack) > methanol (1 kWe/ref-stack). To meet all the power shortage, hydrogen-based plants have the smallest sizing factor, followed by syngas, methane and methanol. Ammonia-based RSOC plant has the highest sizing factor.

The plant designs affect (1) the sizing factor, (2) energy conversion efficiencies, thus the chemical purchase costs and sale profits. The variation of chemical purchase costs with different wind electricity penetrations and plant concepts is analyzed below.

5.1.3. Profit breakdown

The profit employed in Eqs. (1) and (2) is further broken down into income and cost contributions as illustrated in Fig. 9. For the case with 150% wind electricity penetration in Fig. 9(a), the annual income (23.7 M€/year) is mainly contributed by the reduction of imbalance costs (R^{imb}), i.e., 19.6 M€/year, with the remaining 17% contributed by the

sale of additional wind electricity accommodated (R^{elec}), i.e., 4.0 M€/year. The two income contributions R^{imb} and R^{elec} remain the same under different process chains and plant numbers, because all the positive deviations, i.e., the electricity needs, are completely addressed by the RSOC plants (Eq. (10)). Thus, with the same wind electricity penetration, the variation of profit between different process chains and plant numbers is only affected by the expenditures related to the chemical trade, and plant startup. It is found that the chemical produced from the PowSto mode is not enough to satisfy the need for the PowGen mode. Overall, chemical purchase costs contribute to over 90% of annual operating costs. The syngas-based pathway realizes the lowest chemical purchase costs (9.1–11.3 M€/year), resulting in the highest profit. The chemical purchase costs of the methane and hydrogen process chains are in 12.5–14.0 and 14.2–17.8 M€/year, respectively. The ammonia pathway has the highest chemical purchase costs 16.2–19.1 M€/year because of the lowest PowSto efficiency, resulting in the lowest profit. The startup costs contribute only 4–9% of the annual costs, 0.8–1.0 M€/year; while the storage tank costs account for only less than 1% due to the strong interactions with the chemical market.

With the increase in wind electricity penetration from 150% to 200%, the annual incomes are still contributed by the reduction of imbalance costs R^{imb} (15.1 M€/year, 83%) and the sale of additional electricity R^{elec} (3.1 M€/year, 17%). Both incomes decrease since more electricity demand can be satisfied by wind power in terms of both capacity and energy. The increased penetration of wind electricity could reduce the chemical purchase costs since more fuel could be produced from the PowSto mode due to increased excess electricity. The chemical purchase costs of the hydrogen pathway drop sharply to 2.5–6.2 M€/year because of saving large amount expensive hydrogen purchase, enabling it to become the most economically feasible. By using syngas, methane and methanol, the chemical purchase costs are decreased to 3.6–6.5, 8.8–10.2 and 9.6–11.0 M€/year, respectively, while the decreases in chemical purchase costs cannot compensate for the reduction of income from R^{imb} and R^{elec} , thus resulting in the reduced profit compared with the scenarios with a wind power electricity penetration of 150%. The chemical purchase costs of the ammonia pathway (8.7–11.2 M€/year) are still higher than those of other pathways, thus its profit remains the lowest.

The chemical purchase costs of each process chain decrease with the increased number of plants installed, as shown in Fig. 9. The increments are at least 1 M€/year (the methane pathway for the wind electricity penetration of 150%) and even 4 M€/year (the hydrogen pathway for the wind electricity penetration of 200%). The high chemical costs when using a single plant will be further investigated below.

Considering the definition in Eqs. (1) and (2), the variation of plant CAPEX target under different plant concepts and wind electricity penetrations as mentioned in Section 5.1 can be investigated based on (1) the profit analyzed above and (2) the sizing factors analyzed in Section 5.1.2. With wind electricity penetration of 150%, the syngas-based plant



(a) Average PowGen and PowSto efficiency

(b) Average specific PowGen and PowSto capacity

Fig. 8. Plant designs selected for the cases with the highest plant CAPEX targets: (a) average PowGen and PowSto efficiency, (b) average specific PowGen and PowSto capacity.

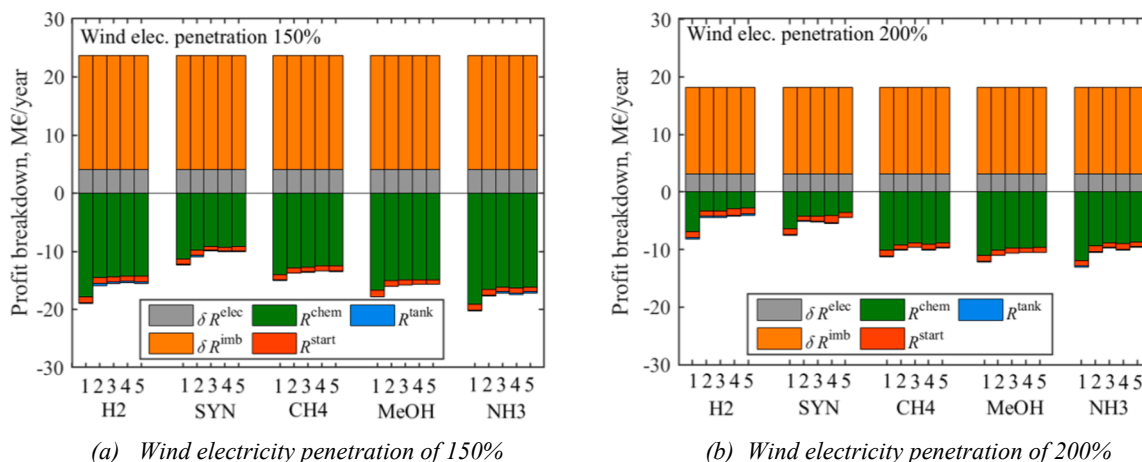


Fig. 9. Annual cost/profit breakdown of different process chains under different scenarios with various plant numbers and wind electricity penetration: (a) 150%, (b) 200%.

has the highest profit and smallest sizing factor hence the largest plant CAPEX target, followed by methane, hydrogen and methanol. The lowest plant CAPEX target in the ammonia process chain is caused by the lowest profit and highest sizing factor.

Increasing wind electricity penetration to 200%, the hydrogen process chain has the highest profit and lowest sizing factor resulting in the highest plant CAPEX target, followed by the syngas process chain. Methane, methanol and ammonia have a low profit while having high sizing factors, leading to low plant CAPEX targets.

5.1.4. Dispatch

The maximum profit is gained by the optimal coordination of multiple plants and different modes. Starting from the case with a single plant installed for the hydrogen pathway with wind electricity penetration of 150% (Fig. 10), the plant capacity is 82 MW for the PowSto mode and 37.2 MW for the PowGen mode. The optimal PowGen capacity is higher than the maximum power shortage to satisfy the application reliability requirement, i.e., all the load demand should be satisfied (Eq. (10)). The power storage is limited by the insufficient PowSto capacity. After reaching the maximum power storage capacity, additional wind power will be curtailed. For this example, 8.6% wind power is lost, which is one factor leading to fuel purchase in the PowGen mode, as mentioned in Section 5.1.3. This lost wind due to the employment of a single plant could be solved by the coordination among multiple plants. For example, for one case with 3 plants with 65 MW PowSto/12 MW PowGen, 39 MW PowSto/18 MW PowGen and 18 MW PowSto/8 MW PowGen, the excess wind electricity curtailed when using a single plant is consumed by dispatching the operation of these three

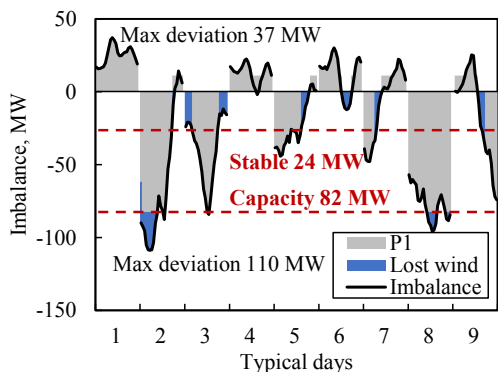


Fig. 10. Dispatch of a single plant for the hydrogen pathway with wind electricity penetration of 150%.

plants. The PowSto capacity range is extended to 5–122 MW, reducing the lost wind rate down to 0.5%. However, the lost wind rate cannot be further decreased by employing more plants. For example, when using 5 plants, the lost wind rate is still 0.5% due to the limit of PowSto stable level, thus the fuel costs and annual earning remain almost unchanged (Fig. 9(a)). However, a capacity oversize is observed when employing 5 plants, which means that the annual full load operating load becomes lower and the hardware is not fully utilized, leading to a reduced plant CAPEX target (Fig. 5(a)), thus a lower economic feasibility. The influences of the numbers of plant on plant CAPEX targets for the process chains enabled by methane, methanol and ammonia are similar to the hydrogen pathway.

For the syngas process chain, the case with one plant tends to allow for a higher plant CAPEX target than the cases with multiple plants, especially with higher wind electricity penetration (e.g., 200%) (Fig. 5 (b)). The syngas process chain has high PowSto efficiency compared with other process chains due to the benefit of co-electrolysis as analyzed in Ref. [25]. The highest plant CAPEX target of the case with a single plant is due to the smallest sizing factor.

5.1.5. Sensitivity analysis

(1) Hydrogen price

The case of hydrogen pathway with the highest plant CAPEX target is further investigated with the most potential syngas-based case given as a

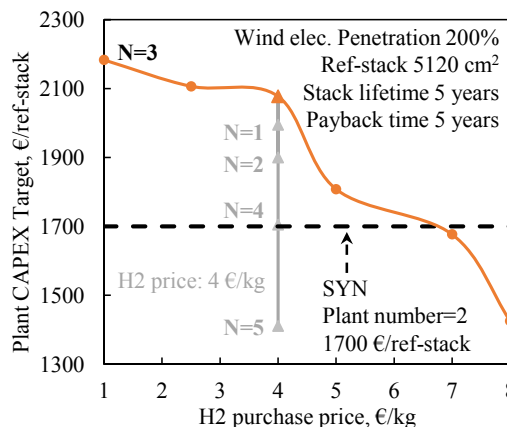


Fig. 11. The effects of hydrogen purchase price on plant CAPEX target with the sale price set as 70% of the purchase price.

comparison. The variation of hydrogen purchase price (1–8 €/kg) is applied to the reference hydrogen-based case with a hydrogen price of 4 €/kg, a plant number of 3 and a wind electricity penetration of 200%. As shown in Fig. 11, with the hydrogen price rising from 1 to 8 €/kg, the plant CAPEX target decreases from 2200 to 1400 €/ref-stack, due to (1) the reduced plant profit caused by the increased costs of hydrogen (from 1.5 to 4 M€/year) to allow for continuous operation of the PowGen mode, and (2) the increased plant sizes to convert more wind power into hydrogen thus reducing the hydrogen purchase. When the hydrogen price is over 7 €/kg, the hydrogen pathway becomes less economically feasible than the syngas process.

(2) Imbalance price and electricity price

The plant CAPEX target of the most potential case, i.e., three plants employed for the hydrogen pathway with wind electricity penetration of 200%, is also evaluated with imbalance price of 195–300 €/MWh [38] and electricity price of 20–100 €/MWh [43] as shown in Fig. 12. The plant CAPEX target decreases at higher electricity or imbalance prices, indicating a high economic feasibility of the RSOC plants. The plant CAPEX target may reach 3400 €/ref-stack if the imbalance price is up to 300 €/MWh and electricity price reaches 100 €/MWh. While, if the imbalance price is down to 195 €/MWh and the electricity price is 20 €/MWh, the profit from addressing the imbalance will be significantly reduced and leading to plant CAPEX target down to 1600 €/ref-stack.

(3) Wind electricity penetration

With the increase in wind electricity penetration up to 250%, the plant CAPEX target of the hydrogen pathway can increase up to 2300 €/ref-stack due to revenue from hydrogen sales, as shown in Fig. 13. The hydrogen pathway remains the most economic potential under high wind power generation and with no big need for hydrogen storage. However, for the syngas, methane and methanol pathways, the plant CAPEX targets reduce down to 1550, 1000 and 900 €/ref-stack, indicating reduced economic feasibility. This is due to that (1) the revenue from the chemical sale cannot compensate for the reduction of revenue from addressing grid imbalance R^{imb} and increasing electricity sale R^{elec} , thus resulting in reduced profit, and (2) the plant sizes is increased to handle the increased excess wind power under a higher wind electricity penetration. The plant CAPEX target of the ammonia process chain also increases with the increased penetration of wind electricity, but the enhancement remains limited. However, its CAPEX target is still over stringent which will not be advocated from the perspective of economics.

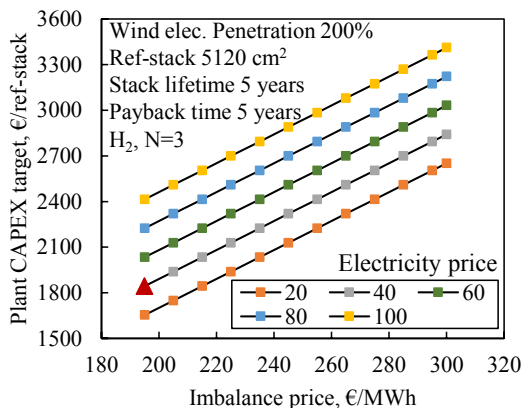


Fig. 12. The effects of imbalance price and electricity price on plant CAPEX target.

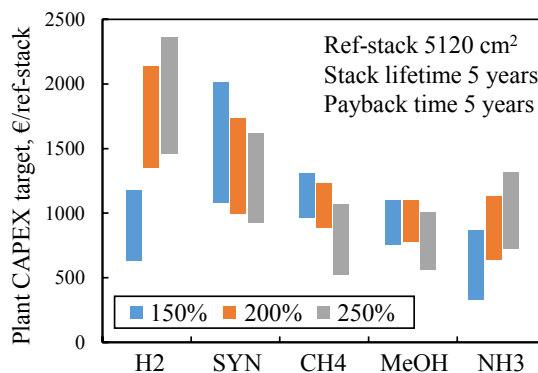


Fig. 13. The variation of plant CAPEX target for the three wind electricity penetrations: 150%, 200% and 250%. The hydrogen price is set as 4 €/kg.

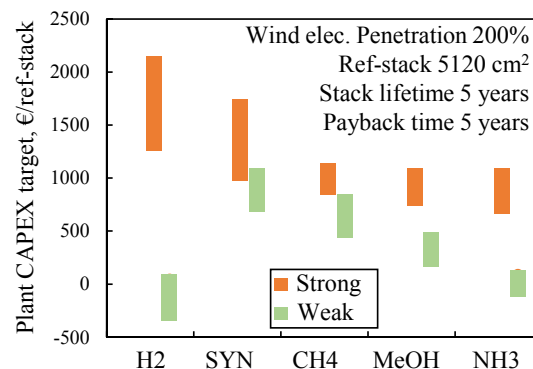


Fig. 14. Plant CAPEX targets under weak interactions with the chemical markets for the scenario with wind electricity penetration of 200%.

5.2. The scenario with weak interactions with the chemical market

The economic feasibility of RSOC plant under weak interactions with the chemical markets is assessed for the scenario with a wind electricity penetration of 200%. The chemicals generated by the RSOC plant are not sold to the market but stored onsite, while the purchase of chemicals is allowed if there is a lack of fuel to drive PowGen mode. Overall, the plant CAPEX targets of all pathways are reduced (Fig. 14), due to the increased onsite storage sizes. The hydrogen pathway drops sharply to $[-300, 50]$ €/ref-stack and becomes not economically feasible any more, because of expensive hydrogen storage (200 €/kg) and hydrogen purchase costs (4 €/kg). The syngas and methane pathways perform better with the increased onsite chemical storage, with their plant CAPEX targets reaching 800–1000 and 500–800 €/ref-stack, respectively. The chemical purchase and storage costs are leveled to around 10 M€/year. The methanol and ammonia pathways, however, present much higher chemical storage and purchase costs of around 14 and 17 M€/year, which makes them not economically feasible as well represented by a plant CAPEX target of 200–400 and 0–100 €/ref-stack. This low plant CAPEX target also results from a higher lost wind rate because (1) the design characteristics do not match well with the imbalance characteristics, and (2) the energy conversion efficiency is lower as analyzed in Section 5.1.2.

6. Conclusions

The economic feasibility of employing dual-direction reversible solid-oxide cell stack based plants for addressing grid imbalance is evaluated via the *Plant CAPEX Target* (€/ref-stack), defined as the maximum affordable plant investment cost, i.e., the maximum affordable total plant investment costs divided by the equivalent number of

reference stacks (each with 5120 cm² active cell area). The dual-direction plant concepts enabled by hydrogen, syngas, methane, methanol, and ammonia, are considered. A decomposition-based optimization methodology has been instantiated and applied to maximize the profits from imbalance handling and chemical trade by varying a set of degrees of freedom including (1) plant design, (2) plant number, (3) plant sizes, (4) plant operation. The evaluation is performed for various application scenarios formed by (1) different levels (strong/weak) of interactions with the chemical market, leading to different sizes of chemical storage tanks, (2) different wind electricity penetration (150%/200%/250%). Among all application scenarios, the plants should ensure the supplement of power shortage for a reliable power system. Major conclusions are.

- With strong interactions with the chemical market, the hydrogen pathway is the most economic potential, particularly under high wind electricity penetration of, e.g., 200%, followed by the syngas and methane pathways, while methanol and ammonia process chains seem to be not economically-competitive for this specific application. With a wind electricity penetration of 200–250%, the plant CAPEX target (€/ref-stack) is ranked as hydrogen (1400–2300) > syngas (1100–1700) > others (700–1400). A further increase in the wind electricity penetration can enhance the economic feasibility of hydrogen and ammonia pathways.
- With strong interactions with the chemical market, the decrease in hydrogen purchase price enhances the economic feasibility of the hydrogen pathway. With a wind electricity penetration of 200%, the plant CAPEX target remains at around 2000 €/ref-stack at a high price below 4 €/kg; while, when it reaches over 7 €/kg, the hydrogen-based pathway becomes less economically feasible than the syngas-based.
- The plant designs with high round-trip efficiencies are generally preferred for deployment, since they could reduce the chemical purchase costs under the wind electricity penetration of even 200%. However, when the grid-interaction characteristics of a plant design match the imbalance characteristics well, it may also be preferred since it could reduce the lost wind rate and compensate for a reduced efficiency.
- Multiple plants are able to enhance the profit by cooperative operation of the plants with different thermodynamic performances. The lost wind rate can be reduced down to 0.5%.
- When the chemicals produced in the power storage mode are not sold to the market, the expensive hydrogen storage capacity increases largely and thus it is no longer economically feasible. The methanol and ammonia pathways also become not economically feasible. The syngas and methane pathway can achieve a plant CAPEX target of 500–1000 €/ref-stack, indicating a strong need for a significant reduction of stack and system CAPEX.

Future work should be carried out to calculate the plant CAPEX based on the process flow diagram and the component sizes of each plant deployed, which should be further compared with the calculated plant CAPEX target to reveal potential business cases.

CRedit authorship contribution statement

Yumeng Zhang: Data curation, Formal analysis, Writing - original draft. **Ningling Wang:** Supervision, Validation, Writing - review & editing. **Xiaofeng Tong:** Writing - review & editing. **Liqiang Duan:** Supervision, Validation, Writing - review & editing. **Tzu-En Lin:** Writing - review & editing. **François Maréchal:** Resources, Software, Writing - review & editing. **Jan Van herle:** Funding acquisition, Resources, Writing - review & editing. **Ligang Wang:** Conceptualization, Methodology, Supervision, Writing - review & editing. **Yongping Yang:** Resources, Funding acquisition, Writing - review & editing.

Declaration of Competing Interest

The authors declare that they have no known competing financial interests or personal relationships that could have appeared to influence the work reported in this paper.

Acknowledgement

L. Wang, and J. Van herle have received funding from the European Union's Horizon 2020 under grant agreement No 826161 (Waste2-GridS), 731224 (BALANCE) and 826234 (Waste2Watts), and support from the Fuel Cells and Hydrogen Joint Undertaking, Hydrogen Europe and Hydrogen Europe research. Y. Zhang has received funding from the Fundamental Research Funds for the Central Universities (2019QN029 and 52090060). Y. Yang has received funding from the National Nature Science Foundation of China (Grant No. 51821004). T.-E. Lin thanks the Young Scholar Fellowship Program by the Ministry of Science and Technology (MOST) in the Republic of China, under Grant MOST 108–2636-E-009–012.

References

- [1] Gandoman F, Ahmadi A, Sharaf A, Siano P, Pou J, Hredzak B, et al. Review of FACTS technologies and applications for power quality in smart grids with renewable energy systems. *Renew Sustain Energy Rev* 2018;82:502–14.
- [2] Díaz-González F, Sumper A, Gomis-Bellmunt O, Villafafila-Robles R. A review of energy storage technologies for wind power applications. *Renew Sustain Energy Rev* 2012;16(4):2154–71.
- [3] (EESI), E., 2020. Fact Sheet: Energy Storage (2019) | White Papers | EESI. [online] Eesi.org. Available at: <<https://www.eesi.org/papers/view/energy-storage-2019>> [Accessed 2 November 2020].
- [4] IEA. Energy Storage, IEA, Paris, 2020. <https://www.iea.org/reports/energy-storage>
- [5] World-nuclear.org. 2020. Electricity And Energy Storage - World Nuclear Association. [online] Available at: <<https://www.world-nuclear.org/information-library/current-and-future-generation/electricity-and-energy-storage.aspx>> [Accessed 2 November 2020].
- [6] Schimpe M, Naumann M, Truong N, Hesse H, Santhanagopalan S, Saxon A, et al. Energy efficiency evaluation of a stationary lithium-ion battery container storage system via electro-thermal modeling and detailed component analysis. *Appl Energy* 2018;210:211–29.
- [7] Energinet. System perspectives for the 70% target and large-scale offshore wind, 2020.
- [8] Nguyen V, Fang Q, Packbier U, Blum L. Long-term tests of a Jülich planar short stack with reversible solid oxide cells in both fuel cell and electrolysis modes. *Int J Hydrogen Energy* 2013;38(11):4281–90.
- [9] Wang Y, Leung D, Xuan J, Wang H. A review on plantized regenerative fuel cell technologies, part B: Plantized regenerative alkaline fuel cell, solid oxide fuel cell, and microfluidic fuel cell. *Renew Sustain Energy Rev* 2017;75:775–95.
- [10] Wang Y, Leung D, Xuan J, Wang H. A review on unitized regenerative fuel cell technologies, part-A: Unitized regenerative proton exchange membrane fuel cells. *Renew Sustain Energy Rev* 2016;65:961–77.
- [11] Grigoriev S, Millet P, Dzhus K, Middleton H, Saetre T, Fateev V. Design and characterization of bi-functional electrocatalytic layers for application in PEM unitized regenerative fuel cells. *Int J Hydrogen Energy* 2010;35(10):5070–6.
- [12] Graves C, Ebbesen S, Jensen S, Simonsen S, Mogensen M. Eliminating degradation in solid oxide electrochemical cells by reversible operation. *Nat Mater* 2014;14(2):239–44.
- [13] Jacobson AJ. Materials for solid oxide fuel cells. *Chem Mater* 2010;22(3):660–74.
- [14] Jensen SH, Graves C, Mogensen M, Wendel C, Braun R, Hughes G, et al. Large-scale electricity storage utilizing reversible solid oxide cells combined with underground storage of CO₂ and CH₄. *Energy & Environ Sci* 2015;8(8):2471–9.
- [15] Mermelstein J, Posdziech O. Development and demonstration of a novel reversible SOFC system for utility and micro grid energy storage. *Fuel Cells* 2017;17(4):562–70.
- [16] Posdziech O, Schwarze K, Brabandt J. Efficient hydrogen production for industry and electricity storage via high-temperature electrolysis. *Int J Hydrogen Energy* 2019;44(35):19089–101.
- [17] Reznicek E, Braun R. Techno-economic and off-design analysis of stand-alone, distributed-scale reversible solid oxide cell energy storage systems. *Energy Convers Manage* 2018;175:263–77.
- [18] Reznicek E, Braun R. Reversible solid oxide cell systems for integration with natural gas pipeline and carbon capture infrastructure for grid energy management. *Appl Energy* 2020;259:114118.
- [19] Guo Z, Ge S, Yao X, Li H, Li X. Life cycle sustainability assessment of pumped hydro energy storage. *Int J Energy Res* 2019;44(1):192–204.
- [20] Akikur R, Saidur R, Ping H, Ullah K. Performance analysis of a co-generation system using solar energy and SOFC technology. *Energy Convers Manage* 2014;79:415–30.

- [21] Yang C, Shu C, Miao H, Wang Z, Wu Y, Wang J, et al. Dynamic modelling and performance analysis of reversible solid oxide fuel cell with syngas. *Int J Hydrogen Energy* 2019;44(12):6192–211.
- [22] Giap V, Kang S, Ahn K. HIGH-EFFICIENT reversible solid oxide fuel cell coupled with waste steam for distributed electrical energy storage system. *Renewable Energy* 2019;144:129–38.
- [23] Wendel C, Braun R. Design and techno-economic analysis of high efficiency reversible solid oxide cell systems for distributed energy storage. *Appl Energy* 2016;172:118–31.
- [24] Butera G, Jensen S, Clausen L. A novel system for large-scale storage of electricity as synthetic natural gas using reversible pressurized solid oxide cells. *Energy* 2019; 166:738–54.
- [25] Wang L, Zhang Y, Pérez-Fortes M, Aubin P, Lin T, Yang Y, et al. Reversible solid-oxide cell stack based power-to-x-to-power systems: Comparison of thermodynamic performance. *Appl Energy* 2020;275:115330.
- [26] Chen B, Hajimolana Y, Venkataraman V, Ni M, Aravind P. Integration of reversible solid oxide cells with methane synthesis (ReSOC-MS) in grid stabilization: A dynamic investigation. *Appl Energy* 2019;250:558–67.
- [27] Zhang Z, Zhou J, Zong Z, Chen Q, Zhang P, Wu K. Development and modelling of A novel electricity-hydrogen energy system based on reversible solid oxide cells and power to gas technology. *Int J Hydrogen Energy* 2020;44(52).
- [28] Rispoli N, Vitale F, Califano F, Califano M, Polverino P, Rosen M, et al. Constrained optimal design of a reversible solid oxide cell-based multiple load renewable microgrid. *J Storage Mater* 2020;31:101570.
- [29] Sorrentino M, Adamo A, Nappi G. Optimal sizing of an rSOC-Based renewable microgrid. *Energy Procedia* 2019;159:237–42.
- [30] Hutter T, Dong S, Brown S. Suitability of energy storage with reversible solid oxide cells for microgrid applications. *Energy Convers Manage* 2020;226:113499.
- [31] Peksen M. Safe heating-up of a full scale SOFC system using 3D multiphysics modelling optimization. *Int J Hydrogen Energy* 2018;43(1):354–62.
- [32] Dietrich R, Oelze J, Lindermeier A, Spitta C, Steffen M, Küster T, et al. Efficiency gain of solid oxide fuel cell systems by using anode offgas recycle – Results for a small scale propane driven unit. *J Power Sources* 2011;196(17):7152–60.
- [33] Fazlollahi S, Bungener S, Mandel P, Becker G, Maréchal F. Multi-objectives, multi-period optimization of district energy systems: I. Selection of typical operating periods. *Comput Chem Eng* 2014;65:54–66.
- [34] Bellotti D, Rivarolo M, Magistri L, Massardo A. Feasibility study of methanol production plant from hydrogen and captured carbon dioxide. *J CO2 Util* 2017;21: 132–8.
- [35] Luckow P, Stanton EA, Fields S, Biewald B, Jackson S, Fisher J, et al. 2015 Carbon Dioxide Price Forecast. Cambridge: Massachusetts; 2015.
- [36] Eia.gov. U.S. Energy Information Administration (EIA) – Qb, 2020. [online] Available at: <<https://www.eia.gov/odata/qb.php?sid=NG.N3045US3.M>> [Accessed 18 September 2020].
- [37] Schnitkey G. Fertilizer Costs in 2017 and 2018. *farmdoc daily*, 7, 2017.
- [38] Zhang Y, Wang L, Wang N, Duan L, Zong Y, You S, et al. Balancing wind-power fluctuation via onsite storage under uncertainty: Power-to-hydrogen-to-power versus lithium battery. *Renew Sustain Energy Rev* 2019;116:109465.
- [39] James BD, Moton JM, Colella WG. Hydrogen storage cost analysis. US DOE Hydrogen and Fuel Cells Program Annual Merit Review, 2013.
- [40] Zhang Z, Zhou J, Zong Z, Chen Q, Zhang P, Wu K. Development and modelling of a novel electricity-hydrogen energy system based on reversible solid oxide cells and power to gas technology. *Int J Hydrogen Energy* 2019;44(52):28305–15.
- [41] Tu H, Stimming U. Advances, aging mechanisms and lifetime in solid-oxide fuel cells. *J Power Sources* 2004;127(1–2):284–93.
- [42] Fuel Cells Bulletin. SOLIDpower expands production capacity, SOFC runtime record. 2017;2017(12):9.
- [43] Unger E, Ulfarsson G, Gardarsson S, Matthiasson T. A long-term analysis studying the effect of changes in the Nordic electricity supply on Danish and Finnish electricity prices. *Econ Anal Policy* 2017;56:37–50.